Conformational Information from Vibrational Spectra of Styrene, *trans*-Stilbene, and *cis*-Stilbene

Cheol Ho Choi and Miklos Kertesz*

Department of Chemistry, Georgetown University, Washington, D.C. 20057-1227

Received: February 19, 1997[⊗]

Two electron correlation theories, second-order Møller−Plesset perturbation (MP2), and density functional (DFT) methods have been adopted to obtain fully optimized structures of styrene, *trans*-stilbene, and *cis*-stilbene. Full geometry optimizations with MP2 shows that the nonplanar conformations of styrene and *trans*-stilbene are preferred by 0.24 (styrene) and 0.80 kcal/mol (*trans*-stilbene), respectively. However, B3LYP, BLYP, and BVWN prefer a planar conformation contradicting the MP2 results. Due to the disorder of the crystal, X-ray experimental data of C═C double bond length of *trans*-stilbene seem to be too short. Vibrational spectra of these molecules are calculated at the BLYP/6-31++G** level without any empirical scaling. The agreement with experiment is excellent, some normal modes are reassigned. The dependence of the IR spectrum as a function of conformation in the 700−800 cm^{-1} region allows the determination of the solution-phase conformation. Both styrene and *trans*-stilbene are planar in solution, implying that these molecular conformations are mainly determined by the *inter*molecular forces rather than *intra*molecular ones.

Introduction

As a prototype of conjugated π-electron system having an aromatic ring and an unsaturated vinyl group, considerable number of experimental[1] and theoretical studies[2,3] have been devoted to styrene. While all experiments have shown the conformation of styrene to be planar, all ab initio calculations[2,3] based on the Hartree−Fock theory (HF) except Bock et al.'s[2b] have suggested that the true minimum is a *gauche* conformation with a torsional angle of about 20° along the bridging bond between the benzene and the vinyl group, although the potential energy surface is very flat along the torsional coordinate. Due to its reactivity, the determination of its structure is difficult and no reliable experimental structural data are available. However, the high quality vibrational data allow us to deduce the conformation of styrene.

More experimental structural studies have been done in the solid[4] and in the vapor phase[5] of *trans*-stilbene which can be considered as a short oligomer of poly(paraphenylene vinylene), PPV, an important conducting polymer.[6] However, while X-ray data and fluorescence studies indicate a near-planar structure for *trans*-stilbene, gas-phase electron diffraction data suggest that both benzene rings are tilted by $\tau = 32.5°$ with respect to the vinyl group. Figure 1 shows the structures of the molecules discussed in this paper. We have chosen the C_2 conformation both for *trans*- and *cis*-stilbene. The other conformation for *trans*-stilbene, corresponding to the C_i point group is nearly degenerate with the C_2 conformation and its vibrational properties are indistinguishable. In the cis case, the other conformation (C_s) is obviously higher in energy due to the $H_3-H_{3'}$ repulsion. Theoretical predictions of torsional angles by HF[2d,7] and semiempirical methods[7a] are in agreement with the electron diffraction data. Treboux et al.[2e] have also reported that the nonplanar conformation of *trans*-stilbene is more stable based on the HUMM (Hückel and molecular mechanics scheme) theory. Furthermore, the only published experimental structural data of *cis*-stilbene obtained by the electron diffraction[8] indicates a strongly nonplanar structure.

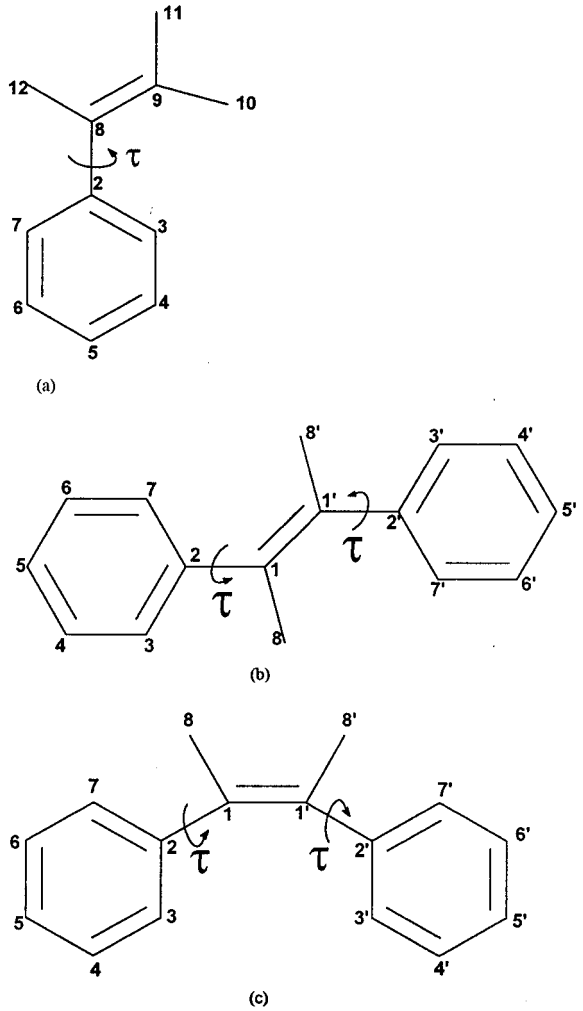

Figure 1. Atomic numbering in (a) styrene, (b) *trans*-stilbene, and (c) *cis*-stilbene.

Conjugated polymers exhibit strong coupling between the electronic structure and certain geometric degrees of freedom.[9]

[⊗] Abstract published in *Advance ACS Abstracts,* May 1, 1997.

S1089-5639(97)00620-8 CCC: $14.00

TABLE 1: Theoretical Geometric Data of Sytrene (Bond Lengths in angstroms, Angles in degrees)[a]

	HF/ 4-21G[b]	HF/ 6-31G[c]	HF/ 6-31G*[b]	BLYP/ 6-31++G**	BLYP/ 6-31++G** [d]	BLYP/ 6-311G(3d,p)	B3LYP/ 6-31G*	MP2/ 6-31G*	MP2/ 6-31G* [e]
C1−C8	1.316	1.327		1.353	1.352	1.345	1.339	1.343	1.343
C1−C2	1.483	1.477	1.480	1.480	1.482	1.479	1.472	1.472	1.472
C2−C3	1.392	1.397	1.394	1.420	1.419	1.414	1.407	1.405	1.406
C3−C4	1.381	1.384		1.403	1.405	1.397	1.391	1.394	1.393
C4−C5	1.385	1.390		1.411	1.409	1.405	1.399	1.397	1.398
C5−C6	1.383	1.386		1.407	1.408	1.400	1.395	1.396	1.395
C6−C7	1.383	1.387		1.406	1.406	1.401	1.395	1.395	1.395
C7−C2	1.391	1.395		1.418	1.418	1.412	1.405	1.404	1.404
C2−C1−C8	126.3	127.6	127.0	127.9	126.5	127.8	127.7	125.3	127.0
C3−C2−C1−C8	21.0	0.0	18.6	0.0	30.0	1.1	0.1	27.2	0
relative energy				0	0.5 [f]			0	0.24[g]

[a] Atomic numbering is defined in Figure 1. [b]Taken from ref 3. [c] Taken from ref 2b. [d] Torsion angle was restricted at 30° during geometry optimization. [e] Molecular planarity has been assumed during geometry optimization. [f] Relative energy as compared with the most stable planar conformation in kcal/mol. [g] Relative energy as compared with the most stable nonplanar conformation is kcal/mol.

Therefore, as model systems for PPV, it is of importance to obtain accurate conformational data for these two molecular systems that will lead to understanding of the electric properties of PPV and other related conjugated polymers.

While ab initio molecular orbital theory has been successfully applied to the internal rotations about single bonds in nonconjugated systems,[10] its extension to the rotations about single bonds in conjugated systems has been a challenge, since partial bond breaking occurs during internal rotations which accompany substantial electron correlation effects. Head-Gordon and Pople[2d] have systemically studied the barriers to internal rotation of dozens of conjugated molecules using single-point second-order Møller−Plesset perturbation energy evaluations at HF optimized geometries and shown that to correctly describe the loss of partial double-bond character upon rotation, the inclusion of electron correlation is necessary. No full-geometry optimization including electron correlation effects has been done on styrene and stilbene.

On the other hand, the vibrational properties of these systems have been rather well studied. For instance, the experimental force field of styrene has been determined by several groups.[11] Hargitai et al.[3] have carried out theoretical predictions of vibrational properties at the HF level in combination with an empirical adjustment of the force constants using the scaled quantum mechanical force field method (SQM)[12] which reproduces the observed frequencies excellently.

Arenas et al.[7c] have recently utilized HF/3-21G frequency calculations combined with the SQM for *trans*-stilbene[13] which resolved most of the earlier discrepancies involving the frequencies, the symmetries and the assignments of fundamental modes. They also proposed a general vibrational assignment for *cis*-stilbene.[14]

The basic assumption behind these theoretical predictions of force fields is the transferability of force constant scaling factors. The empirical scaling factors for styrene and stilbene have been derived from smaller systems. Since five new internal coordinates appear relative to benzene or ethylene, Arenas et al.[7c] could not obtain a complete set of the scaling factors for stilbene. They have adjusted the scale factor related the C−X stretching to 0.92 to reproduce the experimental frequencies at 1264 and 1193 cm^{-1} and arbitrarily assigned a value of 0.80 to the remaining ones. This procedure may affect the band assignments of *trans*-stilbene and also *cis*-stilbene.

Mannfors[13g] has also predicted the vibrational frequencies of planar and nonplanar of *trans*-stilbene concluding that the structure is nonplanar. Since his method was based on the empirical force field and lacked intensity information, in our opinion, this conformational conclusion carries a large inherent uncertainty.

In this paper, two widely used correlation methods have been utilized: MP2 (second-order Møller−Plesset perturbation) and density functional theory (DFT). Recently, DFT has shown impressive performance in the predictions of molecular properties especially, vibrational properties.[15] However, one has to note that its model exchange-correlation functional dependencies make it difficult to devise any systematic way to improve the predicted results.

The full-geometry optimizations with MP2 and DFT in combination with various basis sets have been done not only to study the molecular planarity of styrene and stilbene isomers but also to obtain reasonable geometric data from first principles. After that, frequency calculations have been performed with DFT to study the vibrational properties and their dependence on the molecular conformation. Since DFT can yield very accurate vibrational frequencies, no force constant scaling has been done.

By comparing the predicted spectra directly with experiment in the solution phase for styrene and *trans*-stilbene, we arrive at conclusions concerning conformations regardless of the relative stability of the two conformations in the gas phase.

Computational Details

All density functional calculations have been performed by the Gaussian 94[16] program where the LCGTO-DFT method is adopted. Vosko, Wilk, and Nusair (VWN)[17] and Lee, Yang, and Parr's (LYP)[18] correlation functionals were used for the local spin and gradient corrected density approximation, respectively. Becke's 1988 (B)[19] and his three-parameter hybrid (B3)[20] exchange functionals were used for the gradient-corrected density approximation. These density functional methods were performed with DZ and TZ basis sets augmented with polarization and diffuse functions. For the frequency calculation, the BLYP/6-31++G** theory has been used.

MP2/6-31G* method has been used in the geometry optimizations. The internal coordinate definitions by Pulay et al.[21] have been adopted for both styrene and stilbene.

Results and Discussion

A. Geometry. The fully optimized geometric data of **styrene** with MP2 and DFT methods are presented in Table 1 and compared with earlier calculations. The vinyl C═C bond length and the phenyl C−C bond lengths are longer with methods including correlation. For comparison, full-geometry optimization of ethylene at the MP2/6-31G* level yields a bond length of 1.336 Å. The experimental value in ethylene is 1.334−1.339 Å;[22] therefore, the predicted vinyl C═C double-bond length by the correlated methods seems to be reasonable.

TABLE 2: Theoretical and Experimental Geometric Data of *trans*-Stilbene (Bond Lengths in angstroms, Angles in degrees)[a]

	AM1[b]	HF/3-21G[b]	HF/3-21G[c]	exp[d]	exp[e]	exp[f]	exp[g]	exp[h]
C1−C1′	1.344	1.325	1.325	1.306	1.300	1.336	1.326	1.329
Cl−C2	1.453	1.477	1.477	1.477	1.478	1.472	1.471	1.481
C2−C3	1.405	1.392	1.386	1.391	1.379	1.401	1.392	1.398
C3−C4	1.392	1.382		1.376	1.375	1.390	1.384	
C4−C5	1.395	1.383		1.373	1.369	1.391	1.381	
C5−C6	1.394	1.385		1.380	1.376	1.394	1.383	
C6−C7	1.394	1.381		1.384	1.382	1.393	1.381	
C7−C2	1.403	1.393		1.392	1.391	1.406	1.397	
C2−C1−C1′	124.9	126.3	126.0	126.3	126.6	126.0	126.4	127.7
C7−C2−C1−C1′	16.9	15.0	27.2	3.3−4.98		5.2	3.6−5.3	32.5

	6-31G*						BLYP				
	HF(C_2)	BLYP	B3LYP	BVWN	MP2	MP2[i]	6-31++G**	6-31++G**[j]	6-311G	6-311G*	6-311G(3d,p)
C1−C1′	1.328	1.362	1.349	1.361	1.352	1.357	1.363	1.361	1.362	1.358	1.356
C1−C2	1.478	1.470	1.466	1.472	1.465	1.471	1.472	1.477	1.474	1.470	1.469
C2−C3	1.393	1.420	1.408	1.420	1.406	1.411	1.421	1.420	1.423	1.417	1.416
C3−C4	1.385	1.403	1.393	1.402	1.394	1.398	1.405	1.405	1.405	1.400	1.399
C4−C5	1.384	1.406	1.395	1.404	1.397	1.403	1.407	1.408	1.407	1.402	1.401
C5−C6	1.387	1.409	1.399	1.407	1.398	1.399	1.411	1.409	1.411	1.406	1.405
C6−C7	1.383	1.401	1.391	1.400	1.394	1.400	1.402	1.404	1.402	1.398	1.396
C7−C2	1.395	1.421	1.409	1.421	1.406	1.409	1.422	1.420	1.423	1.419	1.417
C2−C1−C1′	126.1	127.4	127.2	127.6	125.0	126.5	127.3	126.0	127.4	127.5	127.4
C7−C2−C1−C1′	23.3	0.1	0.1	0.1	26.6	0.0	0.0	30.0	0.0	0.0	0.0
MP2 energy					0.0	0.80					

[a] Atomic numberings is defined in Figure 1. [b] Taken from ref 7a. [c] Taken from ref 7c. [d] Taken from ref 4a. [e] Taken from ref 4b. [f] Taken from ref 4c. [g] Taken from ref 4d. [h] Taken from ref 5a. [i] Molecular planarity has been assumed during geometry optimization. [j] Torsion angle were restricted at 30° during geometry optimization.

Since the fully optimized geometries with correlation methods are quite different from those with HF theory, single-point energy evaluations with correlation methods at HF optimized geometry are somewhat uncertain. The most striking discrepancies are seen for the torsional angle, $\tau_{C3-C2-C1-C8}$. While other HF methods yield torsional angles of about 20°, Bock et al.[2b] have obtained a planar conformation at the HF level. As Hargitai et al.[3] have argued, this result is probably due to incomplete optimization. Interestingly, near planarity of styrene can also be seen in the DFT results. However, MP2 theory exhibits a much larger torsional angle, 27.2°. Consequently, the C2−C1−C8 angle is slightly reduced to 125.3°, which is in excellent agreement with the only experimentally determined corresponding angle, 125.6°. If we assume that the MP2 results are the most reliable in Table 1, then DFT seems to be inappropriate for the accurate prediction of the torsional angle. Since the nonplanarity mainly arises from the steric hindrance of the system, current DFT exchange-correlation functionals might not behave correctly in the regime of long-range nonbonded interactions. The relative energy of the planar conformation as compared with the nonplanar conformation is very small, about 0.24 kcal/mol which is practically the same as the value of 0.21 kcal/mol by Head-Gordon and Pople using the MP2/6-311G*//HF/6-31G* model. Furthermore, the π-conjugation indicator, the vinyl C1═C8 bond length, and even the bridging C1−C2 single-bond length are not altered by the conformation change. This implies that a 27° nonplanarity does not reduce π-conjugation significantly. Full-geometry optimization data with BLYP/6-31++G** at fixed torsional angle of 30° are also included in Table 1. Again, no noticeable change in geometry can be found with respect to torsional angles. The calculated relative energy at 30° torsional angle with BLYP/6-31++G** level is 0.5 kcal/mol higher than that of at the planar conformation.

Generally, it can be seen that all bond-length parameters of styrene as calculated with the BLYP method are longer than those with MP2. As the size of basis set is increased to 6-311G(3d,p), all predicted bond lengths are somewhat reduced and become very similar to the MP2 values.

TABLE 3: Theoretical Geometric Data of *cis*-Stilbene (Bond Lengths in angstroms, Angles in degrees)[a]

	HF/ 3-21G[b]	HF/ 6-31G	BLYP/ 6-31++G**	MP2/ 6-31G*	exp[c]
C1−C1′	1.324	1.332	1.365	1.356	1.334
C1−C2	1.484	1.482	1.482	1.478	1.489
C2−C3	1.390	1.395	1.420	1.408	1.398
C3−C4	1.383	1.386	1.404	1.398	
C4−C5	1.384	1.387	1.410	1.402	
C5−C6	1.385	1.388	1.408	1.400	
C6−C7	1.382	1.386	1.406	1.401	
C7−C2	1.390	1.395	1.420	1.407	
C2−C1−C1′	128.3	129.6	131.3	126.8	129.5
C3−C2−C1−C1′	44.7	43.0	33.8	42.4	43.2

[a] Atomic numbering is defined in Figure 1. [b] Taken from ref 7c. [c] Taken from ref 8.

Theoretical and experimental geometric data for *trans*-stilbene are presented in Table 2. During geometry optimizations, C_2 molecular symmetry has been applied for the nonplanar conformations. Since stilbene is expected to have stronger π-conjugation than styrene, the bond length of the double bond of the vinyl group (C1−C1′) of stilbene should be longer than that of styrene. This fact can be seen by comparing the predictions of the same quality of theory in Tables 1 and 2. However, the experimental C1−C1′ bond length is in the range 1.300−1.336 Å, which is about 0.02 Å shorter than the values obtained by any of the methods that include correlation. Therefore, these experimental C1−C1′ bond length values appear to be too short. This bond shortening is likely due to disorder in the crystal.[4]

Again, while all DFT calculations show near planar conformations, the HF and MP2 theories predict large torsional angles that agree with the results of the gas-phase electron diffraction experiment. As we have seen in the styrene MP2 energy comparison, the energetic stabilization by nonplanarity is small, 0.8 or 0.4 kcal/mol per each phenyl ring. This small stabilization is about twice per phenyl ring as compared with that of styrene. Mannfors'[13g] molecular mechanics calculation gives a 0.3 kcal/mol stabilization of the $\tau = 22°$ conformer over the planar one.

TABLE 4: Theoretical and Experimental Vibrational Frequencies of Styrene (in cm^{-1})

	exp						this work			
	CL[a]		MQ[b]				BLYP/6-31++G**		calc	
	IR	Raman	IR	Raman	Wilson[c]	HR[d]	planar	nonplanar[e]	Palmo[f]	Hargitai[g]
CH_2 asym st	3105	3107	3080	3090	3106		3160	3158	3098	3113
ring CH st	3090	3091	3060	3063	3091		3122	3121	3078	3089
ring CH st	3084			3057	3084		3113	3113	3072	3080
ring CH st	3061	3061			3061		3104	3105	3069	3068
ring CH st		3055			3055		3095	3095	3065	3057
ring CH st	3029		3028		3029		3088	3088	3064	3050
CH_2 sym st	3010	3009	3010	3010	3009		3080	3076	3053	3045
CH st	2982	2981	2980	2982	2981		3059	3059	3010	3030
C═C st	1630	1630	1631	1631	1630		1628	1627	1628	1639
ring C−C st	1601	1600	1602	1604	1600		1583	1583	1606	1612
ring C−C st	1575	1575	1577	1576	1575		1558	1557	1585	1585
ring C−H ipb[h]	1494	1495	1497	1491	1494		1483	1481	1496	1499
CH_2 scissoring, ring C−H ipb	1450	1449	1450	1451	1450		1442	1438	1451	1457
CH_2 scissoring	1412	1411	1415	1413	1411		1416	1414	1414	1432
ring C−H ipb	1334	1334	1337	1333	1334		1329	1327	1328	1344
CH rock		1303	1317	1317	1303		1324	1317	1314	1312
CH rock, C−C str	1289		1290	1304	1289		1288	1284	1289	1272
C−C st	1202	1203	1208	1203	1203		1192	1190	1185	1204
ring C−H ipb	1182	1180	1180	1181	1181		1176	1174	1172	1190
ring C−H ipb	1155	1156	1156	1157	1156		1156	1156	1161	1168
ring C−C st	1083	1083	1083		1083		1081	1078	1086	1089
CH_2 rock, ring C−C st	1032	1032		1032	1032		1026	1026	1034	1037
CH_2 rock, ring C−C st	1019	1020	1021	1020	1019		1010	1011	1028	1022
trigonal def		999		1001	999	1001	981	987	1003	998
antisym def	776	775		774	776	775	763	759	781	770
antisym def	623	620		647	621	621	615	615	623	622
antisym def, XCY def	554	554	615	617	553	553	545	551	561	548
antisym def, XCY def		442	438	437	437	437	436	404	433	439
C−X ipb, XCY def		241	237	237	228	228	229	227	232	231
C═C torsion, CH wag	992		990		992		994	981	1001	1003
ring C−H opb[i]	983	987		988	985		961	961	990	984
ring C−H opb			980		970		944	944	966	965
ring C−H opb	909	909	905	911	909		895	895	916	932
CH_2 wag	909	909		905	909		885	890	906	909
ring C−H opb	841	841	840		841		823	826	845	831
puckering ring C−H opb	776	775	775		776		768	769	780	771
ring C−H opb, puckering	698	700	695		699		686	686	701	684
puckering		640	553	558	640		632	639	638	627
antisym torsion	434	431	450	454	433		434	459	440	426
antisym torsion′		407	400		399	399	401	402	406	397
ring antisym torsion, CX ipb		212	214		199	199	203	182	215	193
C−C torsion					38	38	65	84	115	43

[a] Taken from ref 11b. [b] Taken from ref 11c. [c] Taken from ref 24. [d] Taken from ref 11d. [e] Torsional angle along C1−C2 bond has been fixed at 30.0° during geometry optimization and frequency calculation. [f] Taken from ref 11e. [g] Taken from ref 3. [h] In-plane-bending. [i] Out-of-plane bending.

The bond length results based on the B3LYP functionals are in agreement with the MP2 calculation. Since the results of BLYP and BVWN functionals are in agreement with each other but not with MP2 or B3LYP, it seems that the geometric data are more sensitive to the exchange functional rather than the correlation functional. This observation implies that the exact exchange mixing[23] is important in obtaining accurate geometric data. It is curious that as the basis set is increased within the BLYP functional, the bond lengths are becoming more similar to the MP2/6-31G* calculations (see Table 2).

Theoretical geometric data of *cis*-stilbene are presented in Table 3. Because of strong van der Waals repulsion between H8 and H8′, all calculations show torsional angles which are in qualitative agreement with the experiment, although the predicted torsional angle by DFT appears to be about 10° too small. Again, the vinyl C═C bond length is increased and C−C single-bond length is decreased with correlated method relative to HF. As compared to the corresponding bond lengths of the MP2/6-31G* results of *trans*-stilbene, both bond lengths are increased in *cis*-stilbene indicating less conjugation.

B. Vibrational Frequencies. Theoretical frequencies for styrene are presented in Table 4 and are compared with the experimental and earlier theoretical data. Since our BLYP/6-31++G** theory shows near-planar conformation, vibrational frequency calculations with this method have been performed not only at fully optimized geometry (planar model) but also at a partially optimized geometry (nonplanar model) where the

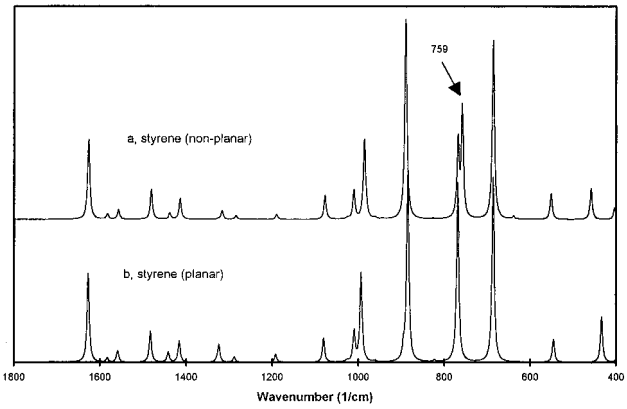

Figure 2. Simulated infrared spectrum of (a) nonplanar and (b) planar models of styrene with BLYP/6-31++G**. All spectra are on the same scale.

torsional angle is fixed at 30.0°. Except the CH stretching region which is usually contaminated by Fermi resonance and large anharmonic contributions, our predicted frequencies by the BLYP method are in excellent agreement with the experiments without empirical force constant scaling.

There is no substantial difference in the vibrational frequencies between our two model conformations of styrene except for a couple of bands. Since the potential energy surface along the torsional coordinate is so flat, this near independence on molecular conformation is not surprising. However, the observed peak around 430 cm^{-1} (433 cm^{-1} according to Wilson[24] and 431 and 434 cm^{-1} according to Condirston and Laposa[11b]) or 450 cm^{-1} (450 and 454 cm^{-1} according to Marchand and Quintard[11c]) is calculated at the near-degenerate values of 434 and 436 cm^{-1} in our planar model. The corresponding splitting becomes 404 and 459 cm^{-1} in our nonplanar model. Although our results with the BLYP/6-31++G** theory should have some inherent error, the 404 cm^{-1} value is clearly too small. Therefore, according to this peak, the results of the planar model are in much better agreement with the experiment than that of the nonplanar model.

The next argument concerns intensities. Infrared spectra of styrene using the two models (planar and nonplanar) have been presented in Figure 2. A strong peak at 759 cm^{-1} appears in the infrared spectrum of the nonplanar model which is absent in the planar model. Recently, we[25] have shown that the DFT method yields quite reliable dipole moment derivatives. *Since we do not see any corresponding peak in the experiment, it can be concluded that in solution, the conformation of styrene is nearly planar regardless of the energetics arguments*. The only question is that if the two peaks around 770 cm^{-1} are accidentally degenerate and do not split as a function of conformation, one still would see only one peak around 770 cm^{-1} and the molecular conformation could still be nonplanar. Condirston and Laposa,[11b] in fact, have assumed the accidental degeneracy for in-plane and out-of-plane modes, both assigned to 776 cm^{-1}. All theoretical studies[3,26] have followed this assignment. They have assumed the planar conformation of styrene in their theoretical model which leads to near-degenerate two peaks with their method. However, according to our calculations which are likely to be more accurate, the two peaks are not degenerate even in the planar conformation.

One of the out-of-plane fundamentals around 950 cm^{-1} was not observed in either IR or Raman. Hargitai et al.[3] have predicted this band at 965 cm^{-1}, in contrast to our value at 944 cm^{-1}. The rest of our assignment is in good agreement with Hargitai et al.[3] except for some minor differences: We assign the observed peaks at 1450 and 1289 cm^{-1} to the mixture of CH_2 scissoring and ring C−H in-plane bending, and vinyl C−H rocking and phenyl C−C stretching modes, respectively. The peaks at 1032 and 1019 cm^{-1} turn out to have more CH_2 rocking contribution than ring C−C stretching. Hargitai et al.[3] have assigned the predicted peaks at 932 and 909 cm^{-1} as CH_2 wagging and ring C−H out-of-plane bending, respectively. According to our results, these two assignments should be switched. Likewise, the assignments of the observed peaks at 776 and 698 cm^{-1} should also be switched.

The root-mean-square errors of the frequencies (excluding C−H bands) of our planar and nonplanar models as compared with Wilson's experiment[24] are 12.7 and 15.9 cm^{-1}, respectively. This result lends further support to our conclusion, that styrene is planar or nearly planar in solution.

The calculated vibrational frequencies of ***trans*-stilbene** are presented and compared with experiments in Table 5. Our two model conformations are a planar model and a nonplanar model where the torsional angle was fixed at 30.0° during geometry optimization. Again, predicted frequencies from both models are in excellent agreement with experiments without scaling, showing small frequency dispersions with respect to the torsional angle. Symmetry assignments correspond to the C_{2h} group and are approximate for the nonplanar conformation.

As we have mentioned in the introduction, Arenas et al.[7c] have adjusted the scaling factor related to the vinyl C−C single bond stretching modes. The overestimation of vinyl C═C bond stretching peak at 1639 cm^{-1} by Arenas et al.[7c] indicates that HF/3-21G does not account sufficiently for the electron delocalization. The fact that the same peak has been underestimated by our BLYP calculations is related to the rather long vinyl C═C double bond. The Raman active peaks at 1338, 1326, and 1289 cm^{-1} are predicted at 1331, 1325, and 1294 cm^{-1} and are assigned to the ring C−C stretching (56%) + C−H rocking (20%), ring C−H in-plane bending (60%), and C−H rocking modes (24%), respectively. Our assignments of these peaks are more or less in agreement with Baranovic et al.[13f] but not with Palmö[13e] and Arenas et al.[7c] They have assigned them in a different order (see Table 5). Although the actual mixing of these modes is different, we have found similar assignments in our styrene potential energy distribution lending further support to our assignments. The infrared-active peaks that were observed at 1332 and 1300 cm^{-1} are predicted at 1326 and 1315 cm^{-1} and are assigned to the ring C−C stretching (44%) + ring C−H in-plane bending (28%) and vinyl C−H rocking (28%) + ring C−C stretching (13%) + C═C stretching (10%) modes, respectively. Arenas et al.[7c] have assigned them quite differently such as C−H in-plane-bending (73%) + vinyl C−H rocking (18%) and ring C−C stretching (69%) + ring C−H in-plane bending (18%), respectively.

Infrared bands at 984, 971, 909, and 847 cm^{-1} and Raman bands at 985, 969, 912, and 838 cm^{-1} have been attributed to the ring C−H out-of-plane bending modes by Arenas et al.[7c] Baranovic et al.[13f] have assigned the Raman band at 969 cm^{-1} to the vinyl C−H wagging mode. According to our results, the infrared band at 966 cm^{-1} is a ring C−H out-of-plane bending mode, while the band at 971 cm^{-1} is a C═C torsion and CH wagging mode. The band at 854 cm^{-1} has been assigned to a fundamental band for the first time by Arenas et al.,[7c] and our results support this assignment.

As we have seen in the case of the styrene, vibrational intensity can be a good indicator of molecular planarity. The infrared spectra of the two models of *trans*-stilbene are presented in Figure 3a,b. Clear intensity differences with respect to the band at 724 cm^{-1} and significant dispersion of the band at 761 cm^{-1} are seen. By lowering the symmetry from C_{2h} (planar) to C_2, the infrared-inactive (but Raman-active) band at 735 cm^{-1} changes to an infrared-active band at 724 cm^{-1}. However, no violation of the mutual exclusion rule occurs in the experiment and the Raman active band at 735 cm^{-1} does not show up in the infrared spectrum. As can be seen from Figure 3, the calculated intensity gain of this band in the nonplanar model is so strong that it could be hardly missed if it was there.

Therefore, similarly to the styrene case, the conformation of trans-stilbene should be planar or nearly planar in solution.

One question arises from our conformational conclusion, though. In fact, nonplanar *trans*-stilbene can have C_i symmetry where the mutual exclusion principle is valid and one would not see the peak around 724 cm^{-1}. Since the energy difference between planar and nonplanar conformation is very small, however, the energy difference between the two nonplanar conformers (C_2 and C_i) should be even smaller. Therefore, the

TABLE 5: Calculated and Observed Vibrational Frequencies of *trans*-Stilbene

				calc[d]			BLYP/6-31++G**		
	exp[a]	exp[b]	calc[c]	planar	nonplanar	calc[e]	planar	nonplanar[f]	
A_g		3082	3078	3082	3081	3084	3122	3121	ring C−H st
			3072	3075	3074	3074	3114	3112	ring C−H st
		3062	3069	3071	3070	3065	3105	3104	ring C−H st
			3065	3065	3064	3054	3095	3094	ring C−H st
		3040	3064	3062	3062	3048	3087	3089	ring C−H st
		3029	3057	3055	3055	3037	3064	3060	C−H st
	1639	1639	1629	1626	1622	1651	1623	1619	C═C st, CH rock
	1594	1593	1604	1599	1597	1616	1574	1576	ring C−C st
	1572	1573	1586	1593	1592	1588	1553	1553	ring C−C st
	1491	1491	1494	1504	1501	1494	1478	1477	ring CH ibp[g]
	1445	1445	1449	1452	1446	1450	1433	1431	ring CH ipb
	1339	1338	1332	1414	1371	1342	1330	1331	ring C−C st
	1327	1326	1310	1329	1326	1319	1326	1325	ring CH ipb
	1292	1289	1295	1301	1298	1299	1302	1294	CH rock
	1193	1193	1182	1205	1193	1193	1179	1178	C−X st, ring C−C st, antisym def
	1187	1184	1171	1180	1181	1189	1175	1173	ring C−H ipb
	1156	1156	1162	1159	1158	1173	1156	1155	ring CH ipb, C−X st
		1093	1083	1087	1084	1083	1075	1072	C−X st
	1027	1026	1031	1037	1036	1027	1017	1017	C−X st
	997	998	1004	1005	1004	994	980	981	ring trigonal def
	868	866	875	887	876	865	856	851	XCY def, ring C−C st
	640	640	653	651	648	645	635	632	antisym def
	617	616	616	613	613	623	614	614	antisym def
	291	336	299	278	329	341	280	339	antisym tor, C−X ipb
	218	198	188	213	183	173	199	168	C−X torsion, C−X ipb
B_u		3095	3078	3082	3081	3084	3122	3121	ring C−H st
		3076	3072	3076	3074	3075	3114	3112	ring C−H st
			3069	3070	3070	3065	3106	3104	ring C−H st
		3056	3065	3065	3064	3055	3095	3094	ring C−H st
		3031	3064	3062	3062	3049	3087	3089	ring C−H st
		3020	3048	3046	3046	3044	3074	3069	C−H st
	1599	1597	1608	1619	1616	1619	1585	1583	ring C−C st
	1577	1577	1587	1593	1591	1592	1558	1556	ring C−C st
	1496	1494	1497	1512	1506	1500	1486	1483	ring, CH ipb
	1452	1450	1453	1444	1442	1455	1442	1437	CH ipb, ring C−C st
	1332	1332	1337	1240	1332	1347	1344	1326	ring C−C st, ring C−H ipb
		1300	1306	1354	1319	1320	1329	1315	C−H rock, ring C−C st, CdbdC st
	1267	1264	1251	1282	1270	1262	1260	1258	C−X st, ring C−C st
	1220	1220	1183	1226	1219	1224	1223	1208	CH rock, C−C st
	1181	1182	1174	1181	1179	1192	1176	1174	ring CH ipb
	1156	1155	1162	1160	1159	1173	1155	1155	ring CH ipb, ring C−C st
	1073	1071	1083	1089	1084	1080	1073	1069	ring C−C st, CH ipb
	1030	1028	1031	1039	1037	1028	1019	1018	ring C−C st
	1002	1001	1004	1005	1005	994	981	982	ring trigonal def
	824	824	816	830	827	812	808	804	ring C−C st
	620	620	623	618	617	625	617	616	anti sym def
	541	541	524	545	540	537	535	530	anti sym def
		419	496	469	493	425	462	418	C−X ipb
			72	90	56	57	79	60	XCY def, phenyl ipb
B_g	985	985	990	984	985	991	962	958	ring CH opb[h]
	969	969	967	961	964	970	942	940	ring CH opb
	916	912	962	919	925	927	931	895	ring CH opb
		854	898	855	864	855	865	838	CH wagging
	842	838	846	839	843	830	821	821	ring CH opb
	735	734	739	723	729	739	729	724	puckering, ring CH opb
		686	692	693	697	693	681	678	puckering
	465	466	466	460	429	502	472	495	C−X opb, antisym tor
	410	412	406	408	410	405	419	400	anti sym torsion
	239	227	250	214	213	212	260	219	antisym torsion, ring CH opb
	132		129	94	127	114	130	123	C−X torsion, antisym torsion
A_u	985	984	990	986	987	992	970	963	ring CH opb, C−X torsion
	972	971	968	976	984	970	953	951	C−X torsion, CH wag
	966	966	946	960	963	956	941	940	ring CH opb
	909	909	912	907	918	922	885	895	ring CH opb
	848	847	845	839	843	831	819	822	ring CH opb
	764	764	764	758	753	766	761	744	puckering, ring CH opb
	693	692	697	695	699	693	681	682	puckering
	528	528	520	528	519	525	546	518	C−X opb
	403	410	405	408	410	405	408	400	antisym torsion
	275	268	288	292	260	257	292	251	antisym torsion, C═C torsion
			59	64	63	55	59	54	C−X torsion
			44	23	29	25	28	23	C−X torsion, C═C torsion

[a] Taken from ref 13c. [b] Taken from ref 7c. [c] Taken from ref 13e. [d] Taken from ref 13g. [e] Taken from ref 7c. [f] Frequency calculation with nonplanar model (see Table 2). [g] In-plane bending. [h] Out-of-plane bending.

TABLE 6: Calculated and Observed Vibrational Frequencies of *cis*-stilbene (in cm^{-1})

		A(C_2)			B(C_2)		
IR[a]	Raman[a]	calc[a]	this work[b]		calc[a]	this work[b]	
3079		3073	3131	ring C−H st	3073	3130	ring C−H st
	3061	3060	3118	ring C−H st	3060	3118	ring C−H st
3054	3049	3047	3106	ring C−H st	3047	3106	ring C−H st
		3040	3096	ring C−H st			
		3036	3088	ring C−H st	3036	3096	ring C−H st
3024	3030	3028	3066	C−H st	3028	3088	ring C−H st
3012	3014				3016	3045	C−H st.
	1629	1656	1609	C═C st			
1600	1599	1615	1578	ring C−C st	1617	1583	ring C−C st
1576	1573	1588	1553	ring C−C st	1591	1556	ring C−C st
1495					1498	1482	ring C−H ipb
1490	1490	1494	1478	ring C−H ipb[c]			
1449					1452	1440	ring C−H ipb, ring C−C st
1444	1443	1448	1432	ring C−H ipb, ring C−C st			
1406	1405				1402	1405	C−H rock
1336	1333	1339	1329	ring C−C st	1336	1325	ring C−H ipb, ring C−C st
	1305	1312	1324	ring C−H ipb, ring C−C st	1295	1300	ring C−C st
	1234	1244	1241	C−H rock, ring C−C st			
1203	1203				1203	1193	C−X st, ring C−C st, C−H rock
	1193	1191	1176	ring C−H ipb	1190	1174	ring C−H ipb
1180	1182	1173	1156	ring C−H ipb	1172	1155	ring C−H ipb
1156	1149	1143	1136	C−X st, ring deformation			
1074		1078	1070	ring C−C st	1082	1075	ring C−C st
1029	1029	1026	1017	ring C−C st	1027	1018	ring C−C st
1001	1001	998	982	antisym def	995	982	antisym def
	992	992	961	ring C−H opb[d]	992	959	ring C−H opb
983		984	952	C−H wag, C═C torsion			
966	965	972	944	ring C−H opb	972	943	ring C−H opb
925					936	904	ring C−H opb
	912	919	896	ring C−H opb			
863	863				861	847	XCY def
844	846	835	827	ring C−H opb	834	824	ring C−H opb
781	782				774	773	C−H wag, ring CH opb, puckering
771	769	776	757	puckering, ring CH opb, C−X opb			
752	752	751	740	ring def, ring torsion			
732	731				724	721	XCY def, C−H wag, antisym def
698	699	695	683	puckering	965	686	ring C−H opb
	682				676	673	puckering
619	619	625	616	antisym def	623	615	antisym def
561	561	557	554	ring torsion, C═C torsion, C−H wag			
519	519	521	512	antisym def, XCY def, C−X ipb			
502					500	498	antisym def
443	449				440	443	antisym torsion, C−X opb
		420	402	antisym tor			
	403	407	392	antisym tor, C═C torsion	403	398	antisym tor
	261	248	257	C−X ipb, antisym tor, XCY def	259	240	C−X ipb
	166	149	156	C−X torsion, C═C torsion, C−X ipb, CH wag	149	153	antisym torsion
		65	73	C−X opb, antisym tor			
		36	28	C−X tor, XCY def	23	23	C−X torsion

[a] Taken from ref 7c. [b] Computed with BLYP/6-31++G** method. [c] In-plane bending. [d] Out-of-plane bending.

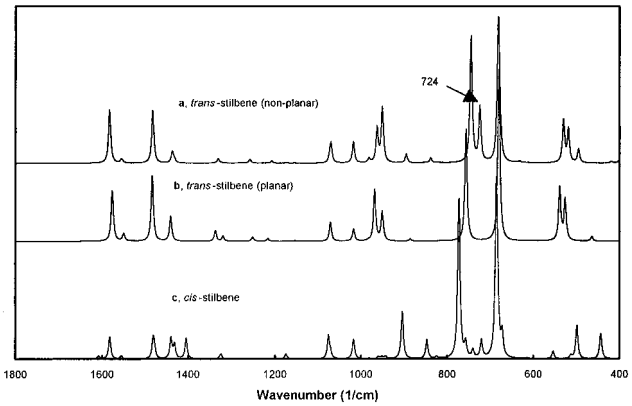

Figure 3. Simulated infrared spectrum of (a) nonplanar *trans*-stilbene and (b) planar *trans*-stilbene and (c) *cis*-stilbene models with BLYP/6-31++G**. All spectra are on the same scale.

abundance of the two nonplanar conformers should be very similar and one should still see the peak around 724 cm^{-1}, if the solution contained a large percentage of nonplanar conformers.

The root-mean-square errors of the frequencies of our planar and nonplanar models as compared with Arenas et al.'s experiment[7c] are 16.4 and 15.4 cm^{-1}, respectively. The difference between the two values is too small to discriminate between the two models.

Theoretical frequencies of ***cis*-stilbene** are presented in Table 6 and compared with experiment. Since the van der Waals repulsion between H8 and H8′ of *cis*-stilbene is strong, there is no doubt that it is nonplanar (C_2 symmetry). Consequently, violations of the exclusion rule in the vibrational spectra are seen.

Unlike *trans*-stilbene, Arenas et al.[7c] have shown that vinyl C−H stretching modes of *cis*-stilbene are computed to be quite far apart from each other, 3040 and 3016 cm^{-1}, respectively. According to our calculation and potential energy distribution analysis, however, experimentally observed peaks at 3024 and 3012 cm^{-1} should be assigned to the vinyl C−H stretching mode, and there is practically no mixing between the vinyl C−H and the benzene C−H stretching modes. These differences in the assignments may be due to the fact that, as they have discussed, the same scale factors and symmetry coordinates were

TABLE 7: Some Selected Diagonal Force Constants of Styrene (in mdyn/Å)

	Palmö et al.[a]	Hargitai et al.[b]	BLYP/6-31++G**	BLYP/6-31++G**[c]
C═C stretching	9.279	8.636	8.629	8.685
C−X stretching	4.701	4.987	4.874	4.804
XCY bending	1.151	1.260	1.315	1.301
C−X rocking	1.135	0.947	0.958	0.862
vinyl C−H rock	0.497	0.554	0.526	0.526
ring C−C stretching	6.561	6.28−6.70	6.114−6.674	6.169−6.619
ring C−H wagging	0.447−0.449	0.429−0.439	0.421−0.445	0.431−0.443

[a] Taken from ref 11e. [b] Taken from ref 3. [c] Nonplanar model.

TABLE 8: Some Selected Diagonal Force Constants of *trans*-Stilbene (in mdyn/Å)

	Palmö et al.[a]	Baranovic[b]	Arenas[c]	BLYP/6-31++G**	BLYP/6-31++G**[d]
C═ stretching	9.279	8.368	8.483	8.063	8.192
C−X stretching	4.701	4.756	4.894−4.972	5.001	4.881
XCY deformation	1.151		0.786−0.846	0.874	0.765
C−X rocking		2.085	0.889−0.908	1.001	0.871
vinyl C−H rock	0.995		0.499−0.565	0.570	0.546
ring C−C stretching	6.601	6.229	6.436−6.762	6.038−6.691	6.120−6.617
ring C−H wagging	0.305		0.304−0.314	0.416−0.444	0.430−0.426

[a] Taken from ref 13e. [b] Taken from ref 13f. [c] Taken from ref 7c. [d] Nonplanar model.

TABLE 9: Some Selected Diagonal Force Constants of *cis*-Stilbene (in mdyn/Å)

	Arenas[a]	BLYP/6-31++G**
C═C stretching	8.641	8.189
C−X stretching	4.739−4.793	4.732
XCY deformation	0.684−1.050	0.932
C−X rocking	0.770−0.798	0.832
vinyl C−H rock	0.535−0.539	0.577
ring C−C stretching	6.648−6.737	6.114−6.577
ring C−H wagging	0.307−0.314	0.429−0.443

[a] Taken from ref 7c.

used as in *trans*-stilbene in their calculations for the *cis*-stilbene which overestimates this coupling and inverts the order.

As in *trans*-stilbene, the assignments of the peaks at 1336 and 1305 cm^{-1} are inverted in our calculation compared with those of Arenas et al.[7c] They have assigned the peaks at 983 and 732 cm^{-1} to the vinyl C−H wagging mode, even though the frequency difference is about 260 cm^{-1}. These assignments are confirmed by our calculation. The rest of our assignments are in good agreement with theirs.

The simulated infrared spectrum of *cis*-stilbene is presented in Figure 3c. Unlike styrene and *trans*-stilbene, the presence of more than one peak in the 700−800 cm^{-1} region is clearly indicating that *cis*-stilbene is nonplanar. This observation is in complete agreement with our argument of the planarity of both styrene and *trans*-stilbene.

C. Force Constants. Some selected diagonal force constants of styrene are presented in Table 7. As compared with those of the planar model, the C═C stretching force constant is increased, while C−X stretching and C−X rocking force constants are decreased in the nonplanar model showing that they are sensitive to the change of π-conjugation between the vinyl group and benzene. Our force cosntants are in better agreement with the SQM results of Hargitai et al.'s[3] than with the empirical force constants of Palmö et al.'s[11e] The corresponding force constants of *trans*-stilbene are presented in Table 8. While the C−X stretching force constant is increased, the C═C stretching and XCY bending force constants are decreased in *trans*-stilbene as compared with the BLYP results of styrene. The increased and the reduced stretching force constants directly reflect the fact that π-conjugation in *trans*-stilbene is stronger than in styrene. Therefore, it is expected that the vinyl C═C bond further increases and the C−X bond decreases in PPV. However, the ring C−C force constants seem to be rather insensitive to the strength of π-conjugation. This observation implies that the π-conjugation between the vinyl group and benzene mainly changes the bond length alternation of the vinyl group and the corresponding force constants. C═C stretching band is observed at 1639 cm^{-1}, while the corresponding band is predicted at 1651 and 1623 cm^{-1} by Arenas et al.[7c] and us, respectively. Therefore, the actual C═C stretching force constant may be between 8.483 and 8.063 mdyn/Å.

The same trend is also found in the *cis*-stilbene force constants (see Table 9), indicating a reduced degree of π-delocalization relative to *trans*-stilbene.

Conclusions

We have presented full-geometry optimizations of styrene and two stilbene isomers at the MP2 and DFT levels of theory. From the results of the correlated calculations, it is seen that geometric parameters are not very sensitive to the torsional perturbation along the bridging bond between the vinyl group and benzene.

Bond length alternation of the vinyl C═C and the C−X bonds is reduced with correlated methods as compared with HF. Geometries except the single-bond torsion, τ, as obtained with B3LYP are in agreement with the results of the MP2 calculations. However, all DFT potentials fail to correctly describe the torsional potential surfaces indicating that the current exchange-correlation functionals might not behave correctly for long-range nonbonding interactions or partial double bond breaking.

Considering the experimental bond length of ethylene and the MP2 results, the vinyl C═C and C−C bond lengths of the X-ray experiments of *trans*-stilbene seem to be unreliable, which should be due to the disorder in the crystal.

Since no significant frequency dispersion occurs with respect to the torsional angle, BLYP/6-31++G** has been adopted in the frequency calculations of styrene and two stilbene isomers without any empirical scaling of force constants. With the help of excellent predictions of vibrational frequencies, new assignments of several bands are proposed. By observing predicted intensity changes of our planar and nonplanar models, we have identified a new band in the IR spectra of styrene and the two stilbene isomers in the 700−800 cm^{-1} region that can be an indicator of planarity. On the basis of this band and other vibrational spectroscopic evidences, we propose that the most probable conformation of styrene and *trans*-stilbene in solution phase is planar regardless of the suggestions of *ab initio*

energetics results which refer to the gas phase. This observation implies that since actual energy barriers of these molecules are small, molecular conformation is mainly determined by the environment in these solutions.

This band may be useful also in obtaining conformational information on a related system such as PPV, which we intend to come back to.

Acknowledgment. We thank the National Science—the National Center for Supercomputing Applications (NCSA, No. DMR-950029N) for the use of supercomputing facilities and the National Aeronautics and Space Administration (NASA, No. 9307-0347) for the funding to Dr. Marko Moskovitch at Georgetown University for the SGI workstation used in this research. Further support by National Science Foundation (NSF Grant CHE-9601976) is also gratefully acknowledged.

References and Notes

(1) (a) Carreira, L. A.; Towns, T. G. *J. Chem. Phys.* **1975**, *63*, 5283. (b) Hollas, J. M.; Ridley, T. *Chem. Phys. Lett.* **1980**, *75*, 94. (c) Hollas, J. M.; Musa, H.; Ridley, T.; Turner, P. H.; Weisenberger, K. H.; Fawcett, V. *J. Mol. Spectrosc.* **1982**, *94*, 437. (d) Caminati, W.; Vogelsanger, B.; Bauder, A. *J. Mol. Spectrosc.* **1988**, *128*, 384.

(2) (a) Schaefer, T.; Penner, G. H. *Chem. Phys. Lett.* **1985**, *114*, 526. (b) Bock, C. W.; Trachtman, M.; George, P. J. *Chem. Phys.* **1985**, *93*, 431. (c) Tsuzuki, S.; Tanabe, K.; Osawa, E. *J. Phys. Chem.* **1990**, *94*, 6175. (d) Head-Gordon, M.; Pople, J. A. *J. Phys. Chem.* **1993**, *97*, 1147. (e) Treboux, G.; Maynau, D.; Malreu, J. P. *J. Phys. Chem.* **1995**, *99*, 6417.

(3) Hargitai, R.; Szalay, P. G.; Pongor, G.; Fogarasi, G. *J. Mol. Struct.* **1994**, *304*, 293.

(4) (a) Finder, C. J.; Newton, M. G.; Allinger, N. L. *Acta Crystallogr.* **1974**, *B30*, 411. (b) Bernstein, J. *Acta Crystallogr.* **1975**, *B31*, 1268. (c) Hoekstra, A.; Meertens, P.; Vos, A. *Acta Crystallogr.* **1975**, *B31*, 2813. (d) Bouwstra, J. A.; Schouten, A.; Kroon, J. *Acta Crystallogr.* **1984**, *C40*, 428.

(5) (a) Traetteberg, M.; Fransten, E. B.; Mijlhoff, F. C.; Hoekstra, A. *J. Mol. Struct.* **1975**, *26*, 57. (b) Chanpagne, B. B.; Pfanstiel, J. F.; Plusquellic, D. F.; Pratt, D. W.; Van Herpen, W. M.; Meerts, W. L. *J. Phys. Chem.* **1990**, *94*, 6.

(6) Burn, P. L.; Holmes, A. B.; Kraft, A.; Bradley, D. D. C.; Brown, A. R.; Friend, R. H.; Gymer, R. W. *Nature* **1992**, *356*, 47.

(7) (a) Lhost, O.; Brédas, J. L. *J. Chem. Phys.* **1992**, *96*, 5279. (b) Langkilde, F. W.; Wilbrandt, R.; Brouwer, A. M.; Negri, F.; Zerbetto, F.; Orlandi, G. *J. Phys. Chem.* **1994**, *98*, 2254. (c) Arenas, J. F.; Tocón, I. J.; Otero, J. C.; Marcos, J. I. *J. Phys. Chem.* **1995**, *99*, 11392.

(8) Traetteberg, M.; Frantsen, E. B. *J. Mol. Struct.* **1975**, *26*, 69.

(9) (a) Brédas, J. L.; Quattrocchi, C.; Libert, J.; MacDiarmid, A. G.; Ginder, J. M.; Epstein, A. J. *Phys. Rev. B* **1991**, *44*, 6002. (b) Masters, J. G.; Ginder, J. M.; MacDiarmid, A. G.; Epstein, A. J. *J. Chem. Phys.* **1992**, *96*, 4768. (c) Libert, J.; Brédas, J. L.; Epstein, A. J. *Phys. Rev. B* **1995**, *51*, 5711.

(10) Hehre, W. J.; Radom, L.; Schleyer, P. v. R.; Pople, J. A. *Ab-Initio Molecular Orbital Theory*; Wiley: New York, 1986.

(11) (a) Pitzer, K. S.; Guttman, L.; Westrum, E. F. *J. Am. Chem. Soc.* **1946**, *68*, 2209. (b) Condirston, D. A.; Laposa, J. D. *J. Mol. Spectrosc.* **1976**, *63*, 466. (c) Marchand, A.; Quintard, J. P. *Spectrochim. Acta A* **1980**, *36*, 941. (d) Hollas, J. M.; Ridley, T. *J. Mol. Spectrosc.* **1981**, *89*, 232. (e) Pietilä, L. O.; Mannfors, B.; Palmö, K. *Spectrochim. Acta A* **1988**, *44*, 141.

(12) Pulay, P.; Fogarasi, G.; Pongor, G.; Boggs, J. E.; Vargha, A. *J. Am. Chem. Soc.* **1983**, *105*, 7037.

(13) (a) Pecile, C.; Lunelli, B. *Can. J. Chem.* **1969**, *47*, 243. (b) Warshel, A. *J. Chem. Phys.* **1975**, *62*, 214. (c) Meic, Z.; Güsten, H. *Spectrochim. Acta* **1978**, *A34*, 101. (d) Meic, Z.; Baranovic, B.; Skare, D. *J. Mol. Struct.* **1986**, *141*, 375. (e) Palmö, K. *Spectrochim. Acta* **1988**, *A44*, 341. (f) Baranovic, B.; Meic, Z.; Güsten, H.; Mink, J.; Keresztury, G. *J. Phys. Chem.* **1990**, *94*, 2833. (g) Mannfors, B. *J. Mol. Struct.* **1991**, *263*, 207. (h) Butler, R. M.; Lynn, M. A.; Gustafson, T. L. *J. Phys. Chem.* **1993**, *97*, 2609.

(14) Bree, A.; Zwarich, R. *J. Mol. Struct.* **1981**, *75*, 213.

(15) (a) Dixon, D. A.; DeKock, R. L. *J. Chem. Phys.* **1992**, *97*, 1157. (b) Fan, L.; Ziegler, T. *J. Chem. Phys.* **1992**, *96*, 9005. (c) Murray, C. W.; Laming, G. J.; Handy, N. C.; Amos, R. D. *J. Phys. Chem.* **1993**, *97*, 1868. (d) Chong, D. P.; A. V. Bree, *Chem. Phys. Lett.* **1993**, *210*, 443. (e) Stirling, A.; Papai, I.; Mink, J.; Salahub, D. R. *J. Chem. Phys.* **1994**, *100*, 2910. (f) Stephens, P. J.; Devlin, F. J.; Chabalowski, C. F.; Frisch, M. J. *J. Phys. Chem.* **1994**, *98*, 11623. (g) Rauhut, G.; Pulay, P. *J. Phys. Chem.* **1995**, *99*, 3093. (h) Johnson, B. G.; Florian, J. *Chem. Phys. Lett.* **1995**, *247*, 120.

(16) Frisch, M. J.; Trucks, G. W.; Schlegel, H. B.; Gill, P. M. W.; Johnson, B. G.; Robb, M. A.; Cheeseman, J. R.; Keith, T.; Petersson, G. A.; Montgomery, J. A.; Raghavachari, K.; Al-Laham, M. A.; Zakrzewski, V. G.; Ortiz, J. V.; Foresman, J. B.; Cioslowski, J.; Stefanov, B. B.; Nanayakkara, A.; Challacombe, M.; Peng, C. Y.; Ayala, P. Y.; Chen, W.; Wong, M. W.; Andres, J. L.; Replogle, E. S.; Gomperts, R.; Martin, R. L.; Fox, D. J.; Binkley, J. S.; Defrees, D. J.; Baker, J.; Stewart, J. P.; Head-Gordon, M.; Gonzalez, C.; Pople, J. A.; Gaussian, Inc., Pittsburgh, PA, 1995.

(17) Vosko, S. H.; Wilk, L.; Nusair, M. *Can. J. Phys.* **1980**, *58*, 1200.

(18) Lee, C.; Yang, W.; Parr, R. G. *Phys. Rev.* **1988**, *B37*, 785.

(19) Becke, A. D. *Phys. Rev.* **1988**, *A38*, 3098.

(20) Becke, A. D. *J. Chem. Phys.* **1993**, *98*, 1372.

(21) Pulay, P.; Fogarasi, G.; Pang, F.; Boggs, J. E. *J. Am. Chem. Soc.* **1979**, *101*, 2550.

(22) (a) Duncan, J. L. *Mol. Phys.* **1974**, *28*, 1177. (b) Duncan, J. L.; Wright, I. J.; Van Lerberghe, D. *J. Mol. Spectrosc.* **1972**, *42*, 463. (c) Hirota, E.; Endo, Y.; Saito, S.; Yoshida, K.; Yamaguchi, I.; Machida, K. *J. Mol. Spectrosc.* **1981**, *89*, 223.

(23) Perdew, J. P.; Ernzerhof, M.; Burke, K. *J. Chem. Phys.* **1996**, *105*, 9982.

(24) Wilson, E. B. *Phys. Rev.* **1934**, *45*, 706.

(25) Choi, C. H.; Kertesz, M. *J. Phys. Chem.* **1996**, *100*, 16530.

(26) (a) Palmö, K.; Mannfors, B.; Pietilä, L.-O. *Spectrochim. Acta A* **1986**, *42*, 1265. (b) Pietilä, L.-O.; Palmö, K.; Mannfors, B. *Spectrochim. Acta A* **1988**, *44*, 141.